unchanged for a monodisperse system. Moreover, a local maximum in the steady-state angle can occur when the statistical average shifts its weight with shear rate from longer rods to shorter rods. Additionally, both the Doi–Edwards and the EEMG models predict a substantially smaller overshoot in the birefringence compared to that measured for flexible systems.

We have also shown that the preaveraging approximation using eq 27 to solve the diffusion equation produces very poor quantitative predictions. It does, however, provide a quick way to estimate the flow properties qualitatively.

In the second part of this series, the DEMG model will be tested against the transient flow results obtained on rodlike collagen proteins using the method of two-color flow birefringence by which fast, transient-flow measurements are possible.

Acknowledgment. This work was supported by the NSF-MRL Program through the Center for Materials Research at Stanford University. Partial support was also obtained from the National Science Foundation (Grant No. NSF-CPE80-25833) and from the ARCO Foundation. In addition, we thank Professor G. Marrucci for his helpful discussion and the preprint of his paper.

References and Notes

(1) Doi, M.; Edwards, S. F. *J. Chem. Soc., Faraday Trans. 2* **1978**, *74*, 560, 918.
(2) Bird, R. B.; Hassager, O.; Armstrong, R. C.; Curtiss, C. F. "Dynamics of Polymer Liquids: Kinetic Theory"; Wiley: New York, 1977.
(3) Chu, S. G.; Venkatraman, S.; Berry, G. C.; Einaga, Y. *Macromolecules* **1981**, *14*, 939.
(4) Zero, K. M.; Pecora, R. *Macromolecules* **1982**, *15*, 87.
(5) Marrucci, G.; Grizzuti, N. *J. Polym. Sci., Polym. Lett. Ed.* **1983**, *21*, 83.
(6) Marrucci, G.; Grizzuti, N. *J. Non-Newtonian Fluid Mech.* **1984**, *14*, 13.
(7) Kuzuu, N. Y.; Doi, M. *Polym. J.* **1980**, *12*, 883.
(8) Doi, M. *Ferroelectrics* **1980**, *30*, 247; *J. Polym. Sci., Polym. Phys. Ed.* **1981**, *19*, 229.
(9) Zebrowski, B. F.; Fuller, G. G., submitted for publication in *J. Polym. Sci., Polym. Phys. Ed.*
(10) Hinch, E. J.; Leal, L. G. *J. Fluid Mech.* **1976**, *76-1*, 187.

Rheooptical Response of Rodlike Chains Subject to Transient Shear Flow. 2. Two-Color Flow Birefringence Measurements on Collagen Protein

Andrea W. Chow and Gerald G. Fuller*

Department of Chemical Engineering, Stanford University, Stanford, California 94305

Donald G. Wallace

Collagen Corporation, Palo Alto, California 94303

Joseph A. Madri

Department of Pathology, Yale University School of Medicine, New Haven, Connecticut 06510. *Received July 30, 1984*

ABSTRACT: Two-color flow birefringence measurements under steady-state and transient shear flow have been obtained on two collagen samples with different molecular weight distributions. The results have been compared to models describing solutions of strongly interacting rodlike polymers, the Doi–Edwards and Doi–Edwards–Marrucci–Grizzuti (DEMG) models, which were studied in detail in part 1 of this two-part series. We have found that only the DEMG model is successful in describing the flow dynamics of the polydisperse collagen solutions. Quantitative comparison of the model to the steady state and the inception of shear results is very good, and the agreement is somewhat poorer with data obtained upon the cessation of shear flow. The quantitative discrepancies in the comparison could be attributed to the finite but limited flexibility of the collagen molecules.

Introduction

The flow response of rodlike and semiflexible polymer chains is of importance to a number of processes utilizing both synthetic and naturally occurring materials to fabricate products with important and unique properties. For example, ultrahigh-strength fibers can be spun from solutions of rodlike aromatic polymer molecules and the possibility of producing such fibers has attracted a great deal of interest from the aircraft and automotive industries.[1] On the other hand, several naturally occurring macromolecules (some proteins and viruses) have rodlike or semiflexible conformations and the flow properties of such systems are also of interest. Collagen protein is one specific example of such a macromolecule which has found application in the fabrication of artificial skin for use in the treatment of burns[2] and as an injectable substance in many cosmetic and reconstructive surgery applications.[3]

The addition of stiff macromolecules in moderate concentration, below any liquid crystalline formation, leads to profound changes in the flow properties of these solutions. Subsequently, there has been a marked increase in the research directed toward understanding the dynamics of rodlike polymer solutions in the semidilute regime. Advances in both experimental and theoretical approaches have been made in recent years, especially with regard to the nature of the interactions between separate chains and

0024-9297/85/2218-0793$01.50/0

their influence on the fluid dynamics. The experimental results reported in the literature, however, mostly involve mechanical measurements either under steady flow conditions or in the limit of linear viscoelasticity. There are very few data on transient flows of large amplitude, and since such flows often offer much more stringent tests of theoretical descriptions of flow processes, it would be of interest to study time-dependent flows.

This paper reports the time-dependent behavior of collagen proteins using a new optical technique, two-color flow birefringence (TCFB), with which very fast, transient flow phenomena can be studied. This is part 2 of a two-part series studying the dynamics of rodlike polymer solutions in semidilute concentrations. In part 1,[4] we have examined two recent molecular theories, the Doi-Edwards model[5] for monodisperse solutions and the Doi–Edwards–Marrucci–Grizzuti (DEMG) model[6] for polydisperse solutions, that describe the dynamics of strongly interacting rigid rods at concentrations below the isotropic–nematic phase transition. In particular, the model predictions of the rheooptical response of such systems to steady-state and transient shear flow were calculated. The numerical solutions indicate that polydispersity plays a very important role on the flow properties especially under transient flow conditions. In addition, we have found that, unlike flexible systems, the rodlike systems exhibit a relatively small overshoot in the flow birefringence following the inception of shear flow even at very high shear rates.

Collagen was chosen for this study primarily because of its rodlike conformation resulting from a triple-helix configuration, although it is an interesting system to study in its own right. The triple-helix conformation that characterizes all collagen molecules is a coil of three polypeptide subunits, or α chains. Each α chain twists in a left-handed helix with three amino acids per turn, and the three chains are wound together in a right-handed superhelix to form a rodlike molecule about 1.4 nm in diameter. The collagen molecule is about 300 nm long.[7]

Collagen does not exist as individual triple-helical molecules in the animal; rather, it packs into ropelike fibrils. In the fibril the molecules undergo spontaneous cross-linking through lysine amino acid side chains. When collagen molecules are solubilized by acid from the fibril, these cross-links remain and result in a polydisperse solution of collagen monomers, dimers, and higher aggregates.

Recent studies[8,9] indicate that the collagen molecule is not perfectly rigid but rather somewhat flexible. Both linear viscoelasticity[8] and sedimentation measurements[9] imply a persistence length of 170 nm for collagen, in comparison with the contour length of 300 nm. On the other hand, a technique using electron micrographs to determine the local curvature and hence the overall flexibility of the collagen molecules indicates a persistence length of about 60 nm.[10] In spite of these somewhat inconsistent results, this protein molecule is nonetheless very stiff when compared with other biopolymers. It has a low level of flexibility with a Young's modulus 40 times larger than that of the double-stranded DNA.[8] Because of its high chain stiffness and the possibility of preparing samples well characterized in molecular weight polydispersity, collagen was chosen as a model system for this study on rodlike chains. Moreover, the collagen solutions are optically transparent and easy to handle in an optical experiment. In this study, we have examined two type I collagen samples with bimodal and trimodal molecular weight distributions. We will compare the flow birefringence results with the DEMG model predictions. The effects of slight flexibility on the flow dynamics of rodlike chains will also be discussed.

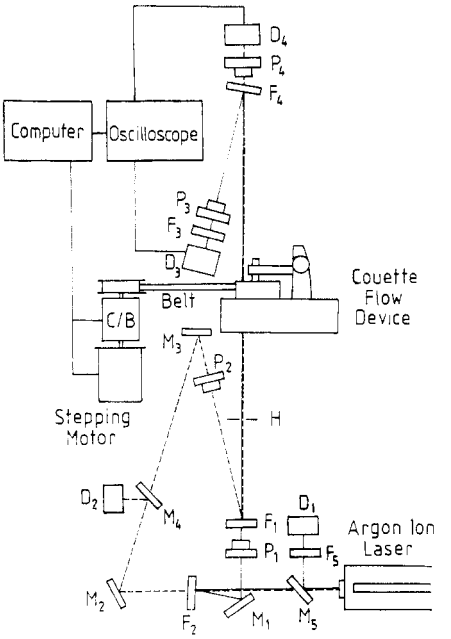

Figure 1. Schematic representation of the TCFB setup: (—) blue light, (– – –) green light. D = photodetector; F = line filter; H = pinhole; M = mirror; P = polarizer.

Experimental Section

Material Preparation and Characterization. Rat Tail Tendon Collagen. The collagen samples were made available to us directly from the Collagen Corp. of Palo Alto, CA. The rat tail tendon collagen was prepared by the method of Chandrakasan et al.[11] The purified solution was then lyophilized and stored below freezing. Final solutions were reconstituted by dissolving the lyophilized samples in 0.01 M HCl followed by addition of glycerin to increase the viscosity for the two-color flow birefringence experiments. The solutions contain 80% of glycerin by volume. A previous study[8] indicates that glycerin does not change the hydrodynamic properties of collagen significantly.

Bovine Collagen. Collagen protein from cowhide was isolated and purified by a modification of the method of Drake et al.[12] The source, bovine corium, was swollen and pulverized in dilute acid, followed by solubilization with porcine pepsin at a weight ratio of pepsin to collagen of 1:100. The solubilized collagen was purified by filtration, ultrafiltration, and, in some cases, ion-exchange chromatography.[13-15] This collagen preparation was characterized as containing no detectable non-collagenous proteins following collagenase digestion (Advanced Biofactures type III, Lynbrook, NY) and examination by polyacrylamide gel electrophoresis[16] in conjunction with the highly sensitive silver staining technique described by Morrissey.[17] Electrophoretic analysis of this material indicated that it was largely type I collagen and contained less than 5% type III collagen.

Because of cross-linking, collagen rods in acidic solution can exist as single rods (monomers) or as two or more rods attached by short telopeptide chains (dimers, trimers, etc.). When solubilization of collagen from tissues is carried out in the presence of pepsin,[12] however, some of the cross-links can be removed. Pepsin is a porcine proteolytic enzyme which cleaves most of the telopeptide chains, but leaves the rodlike helix intact. A portion of the telopeptides survive the pepsin treatment even after exhaustive digestion, however. The result is that polymeric species still remain. Under the denaturing conditions of the electrophoresis experiment, the bovine collagen exhibited α, β, and γ chains, as well as some higher aggregates. β and γ chains are derived from cross-linked native triple-helical molecules. Fragments smaller than α chains represented less than 5% of the total collagen. The amino acid composition of the collagen provided

two residues of tyrosine per thousand residues, indicating about 70% removal of telopeptides.

Collagen in acid solution at 3 mg/mL was then precipitated in 0.02 M sodium phosphate at pH 7.2. The fibrillar precipitate was harvested by centrifugation at 17000*G* and redissolved by dialysis vs. 0.01 M HCl. Purified preparations were held in 0.01 M HCl at 5 °C, either after submicron filtration or in traces of sodium azide. The final solutions used for the TCFB experiment were prepared by adding 80% glycerin by volume to the purified collagen solutions to increase the viscosity.

Determination of Concentration. The concentrations of the final solutions were determined by the Biuret method[18] with a Gilford 2500 spectrophotometer at a wavelength of 550 nm. Preliminary experiments on standard solutions have been done to ensure that glycerin does not affect the measurements.

Determination of Polydispersity. Although high-pressure liquid chromatography and polyacrylamide gel electrophoresis were carried out on denatured collagen chains (α chains), these techniques are of limited use for native (triple-helical) collagen for polydispersity determination. It is difficult to apply sizing chromatographic techniques to native collagen because of the very high molecular weight (monomers: 300 000; dimers: 600 000; etc.).

The best method for determining polydispersity appears to be direct visualization by transmission electron microscopy. With the technique of rotary shadowing it is possible to discriminate monomeric, dimeric, and higher collagen aggregates.[19]

The rotary shadowing technique was adapted from Shotton et al.[20] as modified by Engel et al.[21] The collagen samples in dilute HCl were diluted to 30, 15, and 3 μg/mL with distilled water and made 70% with respect to glycerin (v/v) yielding final concentrations of 10, 5, and 1 μg/mL. The solutions were then sprayed with an airspray over freshly cleaved mica chips at a distance of 20 cm. The chips were then mounted onto a motor-driven horizontal table rotating at 120 rpm in a vacuum chamber. At a vacuum of 2.0×10^{-5} torr the samples were shadowed with platinum–carbon at a 6° angle, followed by carbon coating at a 90° angle. Replicas were floated off the mica chips in distilled water, washed, and picked up on 300 mesh copper grips. Samples were viewed with a Phillips 300 electron microscope at 60 kV using a 30-μm objective aperture. Photographs were taken on Kodak 4463 EM film.

Ten representative fields of each collagen sample were photographed and printed at a final magnification of 75000 ×. A 5 × 5 cm grid network was overlaid and the numbers of monomeric, dimeric, and trimeric species were counted. Counts were made at several concentrations in order to rule out monomer overlap being falsely counted as dimer or trimer species.

Rheooptical Measurements. The measurement of flow-induced optical anisotropy in the form of birefringence has been used for many years in order to probe conformational changes resulting from hydrodynamic forces. Optical techniques such as the flow birefringence are advantageous to methods using mechanical devices for stress measurements. Mechanical devices are often limited in response time by the inertia of their mechanical components, which sometimes even distort the measured signals. Moreover, these measurements are usually averages over a large surface such as the surface of the flow device and therefore not suitable for inhomogeneous flow studies. In contrast, optical measurements are nonintrusive, more localized, and capable of much faster response times. In spite of these advantages, however, the flow birefringence technique has been restricted to steady-state flows in the past. It has only been recently that schemes have been proposed to extend this technique to time-dependent flows. The two-color flow birefringence (TCFB) technique was the first proposed scheme that allows simultaneous determination of the flow-induced birefringence Δn and orientation angle χ with a single measurement. The only two previous methods which have been used for transient flows (Gortemaker et al.,[22] Osaki et al.[23]) require at least two dependent experiments to obtain these two unknowns.

The technique of TCFB has been reported in detail in ref 24 and thus only a brief summary which includes recent modifications of the setup is presented here. The principle behind TCFB is the use of an argon ion laser by which two intense light beams separated in wavelength by 26.5 nm (green and blue) can be generated. Using a unique optical setup as shown in Figure 1, one can effectively perform two flow birefringence experiments

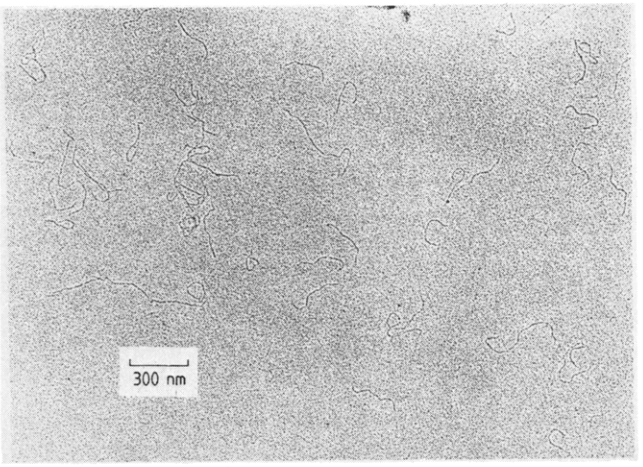

Figure 2. Photomicrograph of a carbon–platinum replica of salt-soluble rat tail tendon collagen. While the majority of the collagen is observed as monomers of 300 nm, there are several dimeric forms noted having contour lengths of 600 nm, consistent with cross-links in terminal regions. In addition, occasional trimeric forms are noted, having contour lengths of 900 nm, again consistent with cross-linking in terminal regions. Rare oligomeric forms are also noted. Original magnification = 75000×.

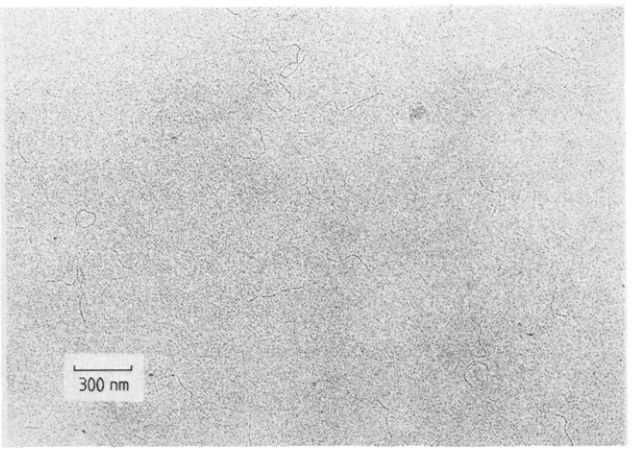

Figure 3. Photomicrograph of a carbon–platinum replica of pepsin-soluble bovine skin collagen. In contrast to the previous figure, the collagen is observed in two forms: the major one being monomeric, having a contour length of 300 nm, and a minor one being dimeric, having contour lengths of 600 nm, consistent with terminal cross-links. No trimeric or oligomeric species were observed. Original magnification = 75000×.

simultaneously, each one using light at a specific wavelength. Illustrated by a dotted line in Figure 1, the 514.5-nm wavelength is selected by a narrow band line filter R_2 and it is directed by mirrors M_2 and M_3 to go through polarizer P_2. This monochromatic, linearly polarized beam is further directed by F_1 to pass through the flow cell. The optical anisotropy of the sample in general interacts with the incident light and changes its state of polarization. The polarization of the transmitted light is then analyzed by a crossed polarizer P_4 (with respect to P_2) and the intensity is measured by photodetector D_4. A similar optical arrangement for another flow birefringence measurement is set up for the 488-nm wavelength (solid line) as the beam is conducted by F_2 and M_1 to pass through polarizer P_1, blue line filter F_1, and finally through the flow cell in coincidence with the green line. The transmitted beam is directed by F_4 toward analyzer P_3 (with respect to P_1) and blue line filter F_3, and the intensity is measured by photodetector D_3. These two simultaneous intensity measurements provide two pieces of information on the anisotropy and the orientation of the polymer sample if the polarizations of the two incident beams are set at two different directions. In our configuration, the polarization directions of P_1 and P_2 are 45° apart. A digital storage oscilloscope (Nicolet 4562) is used to record the two intensity wave forms, and the unknown birefringence and

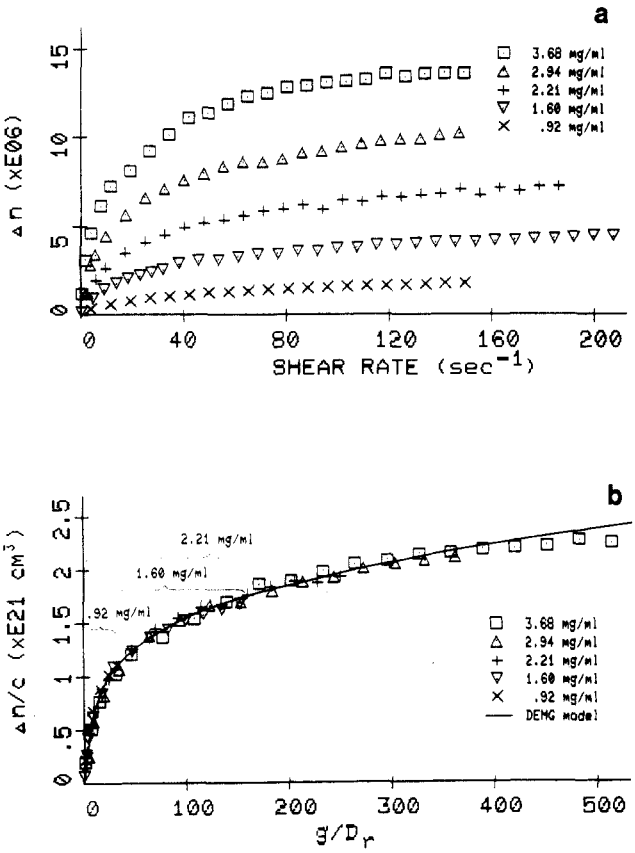

Figure 4. (a) Steady-state birefringence vs. the applied shear rate for five rat tall tendon collagen solutions. (b) Same set of data reduced by the concentration scaling suggested by the DEMG model.

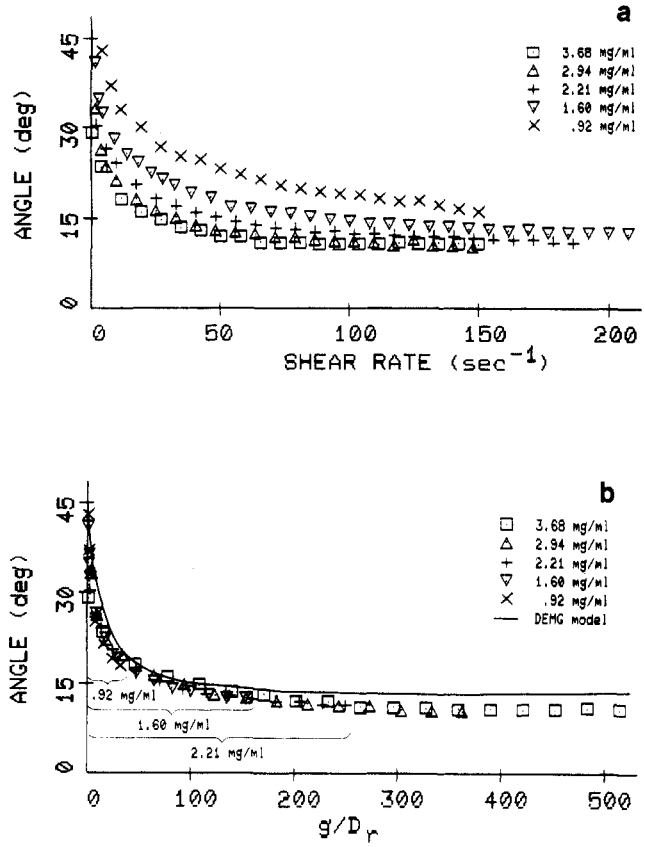

Figure 5. (a) Steady-state orientation angle vs. the applied shear rate for five rat tail tendon collagen solutions. (b) Same set of data reduced by the concentration scaling suggested by the DEMG model.

angle of orientation of the sample can be determined from the data at time scales as fast as 5 ms. Two photodetectors, D_1 and D_2 for blue and green light, respectively, which were not included in the original setup, have been added to measure the incident intensities simultaneously in order to eliminate any uncertainty due to variations in the laser power output. The entire experiment including the flow dynamics of a Couette cell, data collection, and data manipulation are computer controlled.

The flow field, generated by the Couette cell consisting of two coaxial cylinders, is a good approximation of a homogeneous, simple shear flow since the gap width, d, between the cylinders (d = 0.5 mm) is much smaller than the dimensions of the cylinders (2.54 cm for the inside diameter of the outer cylinder). For transient flows, the outer cylinder is set in motion by a synchronous stepping motor through a coupling electromagnetic clutch/brake module. The motion of the cell boundary can therefore be described as a step change in the angular velocity. The flow initiation time, τ, needed for the fluid motion to achieve steady state is generally approximated by the Newtonian limit

$$\tau = d^2/\nu \tag{1}$$

where ν is the kinematic viscosity of the solution. When the solution response time is much longer than the flow initiation time (which is the case for the data reported here), the fluid motion has been assumed to simulate a step change in shear rate. The validity of this assumption has been tested and confirmed by using solutions of different concentrations. A more detailed discussion on the Couette flow development can be found in ref 25.

The transient flow experiments followed a programmed schedule similar to the one described in ref 24. Such a schedule is needed for signal averaging to enhance the signals. The computer first sets the stepping motor at a chosen speed and direction. Next, it sends out a signal that simultaneously engages the electromagnetic clutch which abruptly initiates the flow field and triggers the oscilloscope to start data collection from the photodetectors. After a scheduled period during which the polymer solution establishes steady state, the computer sends out another signal to engage the electromagnetic brake to stop the flow instantaneously. Another duration long enough for the system to completely relax back to the isotropic state is allowed before the computer repeats the same schedule by sending out another signal to engage the clutch and so on. The signal averaging is performed by the oscilloscope and the intensity measurements are transferred to the computer at the end of the experiment. Normally the signals were averaged 3–10 times for the collagen solutions depending on the noise level. All the experiments were performed at room temperature, about 24 °C.

For TCFB, it is important to ensure that dispersion of the birefringence of the sample is small near the wavelengths of the incident beams. Measurements by Oriel and Schellman[26] indicate that dispersion for collagen solutions at 488 and 514.5 nm is 5%, which results in an error of <2.5% for Δn when dispersion is not taken into account.

Experimental Results

Transmission Electron Microscopy (TEM). Figures 2 and 3 are the transmission electron micrographs of the rattail tendon and bovine collagen, respectively. The rattail tendon collagen was found to be trimodal in molecular weight distribution containing 78% monomers, 20% dimers, and 2% linear trimers. Since numerical solutions using the DEMG model indicated that a small amount of the high molecular weight component can affect the flow properties of the solution significantly,[4] the trimers cannot be considered negligible. The bovine collagen, on the other hand, is bimodal in molecular weight containing 85% monomers and 15% dimers. No trimers or higher aggregates were found in this sample.

Two-Color Flow Birefringence (TCFB). Rat Tail Tendon Collagen—Trimodal System. Steady-state and transient flow measurements have been performed on five

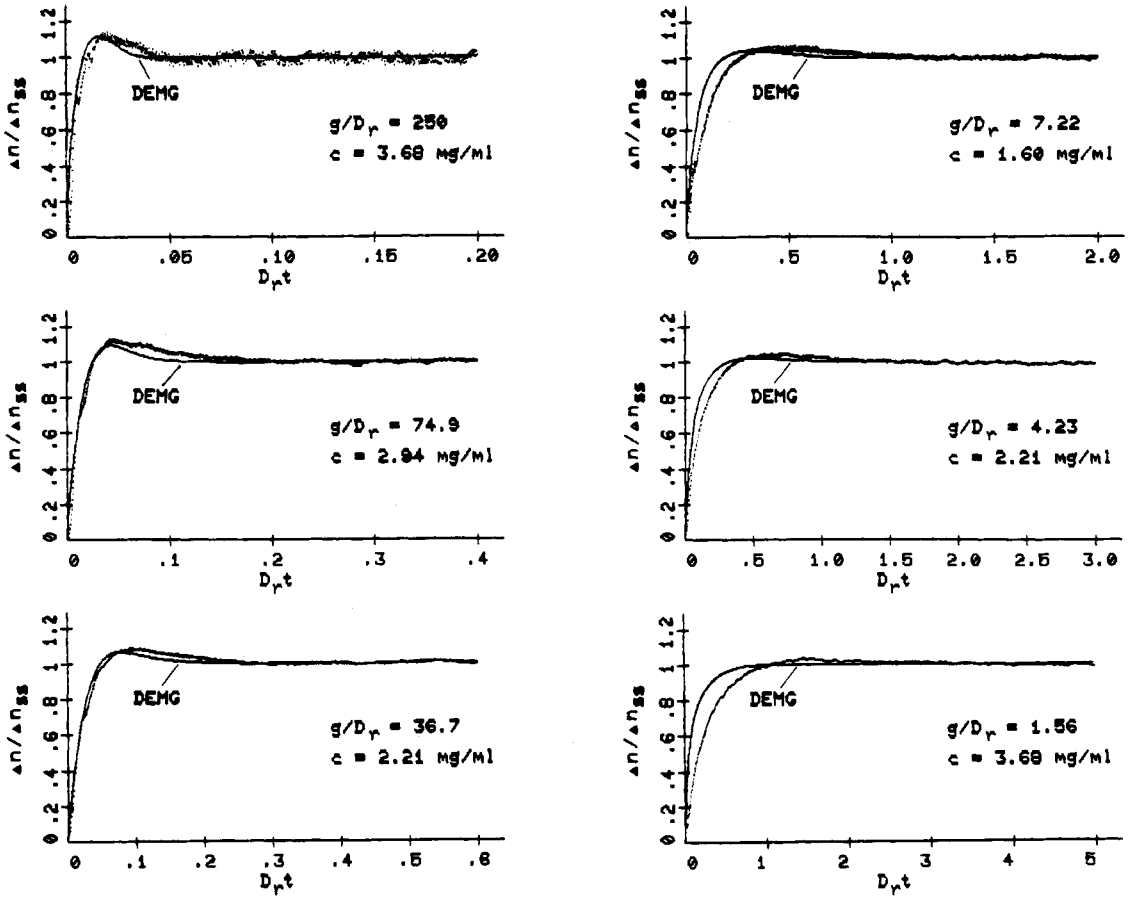

Figure 6. Birefringence normalized by the steady-state value as a function of the dimensionless time following the inception of shear flow for the rat tail tendon collagen solutions. The lines denoted by DEMG are the model calculations.

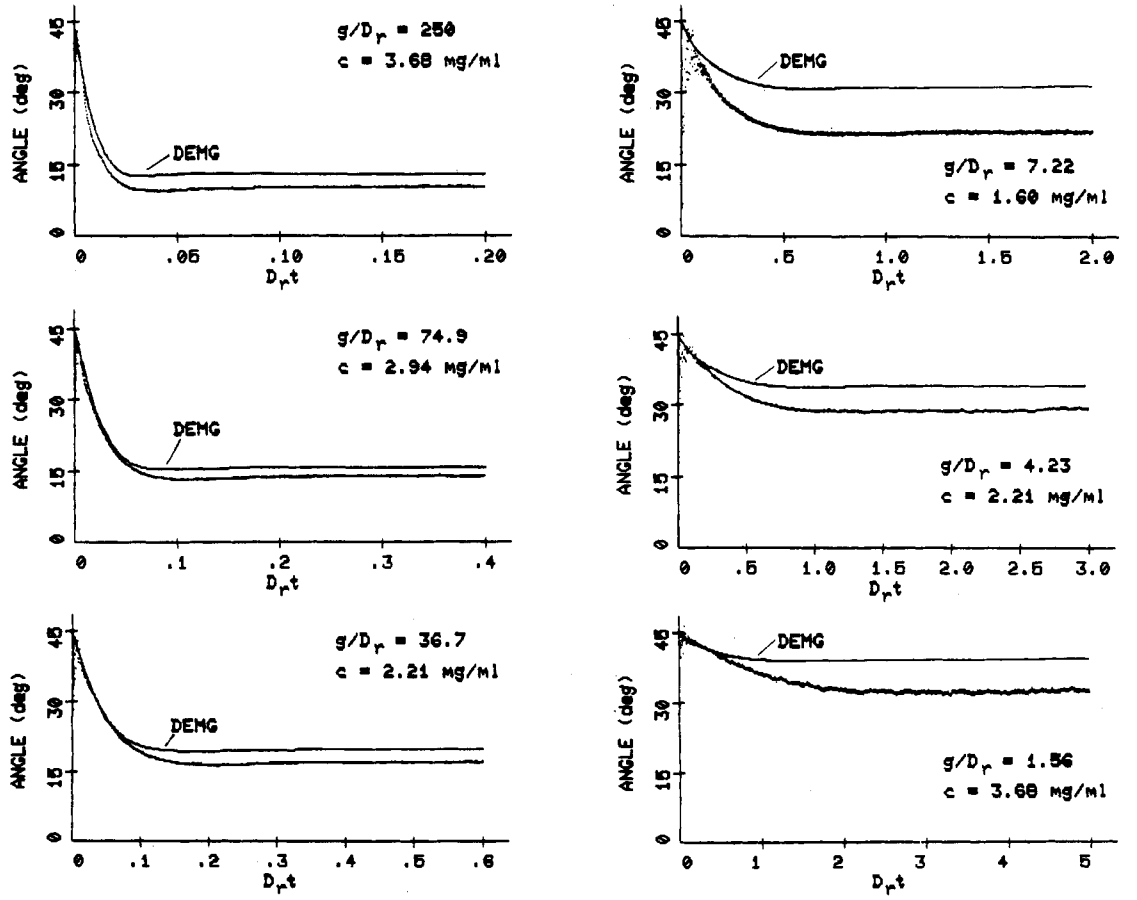

Figure 7. Orientation angle as a function of the dimensionless time following the inception of shear flow for the rat tail tendon collagen solutions. The lines denoted by DEMG are the model calculations.

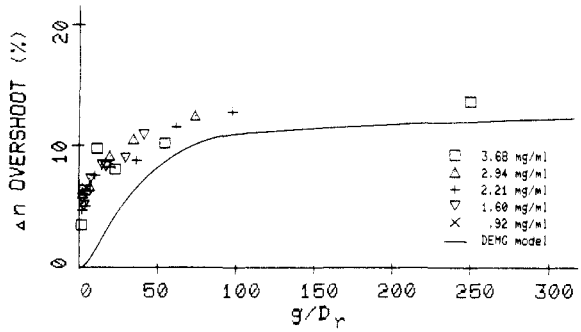

Figure 8. Percent overshoot in birefringence upon the inception of shear flow vs. the dimensionless shear rate for the rat tail tendon collagen solutions.

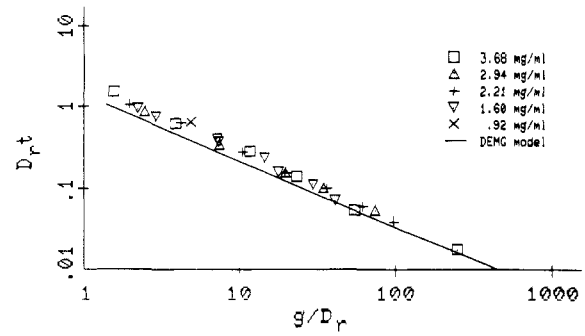

Figure 9. Double-logarithmic plot of the temporal positions of the overshoot in birefringence upon the inception of shear flow vs. the dimensionless shear rate for the rat tail tendon collagen solutions.

rat tail tendon collagen solutions at concentrations between 0.92 and 3.68 mg/mL. Figure 4a shows the steady-state flow birefringence as a function of shear rate for the five solutions, and Figure 5a is the corresponding orientation angle plot. The Doi–Edwards model suggests that if the shear rate g is normalized by the rotational diffusivity D_r, which is proportional to c^{-2}, and the time t is normalized by D_r^{-1}, then both the steady-state and the transient flow data for all concentrations should fall onto two sets of curves as follows:

$$\Delta n/c = Mf_1(g/D_r,D_rt) \tag{2}$$

$$\chi = f_2(g/D_r,D_rt) \tag{3}$$

Here, f_1 and f_2 are two universal functions unique for a specific molecular weight distribution, and M is a proportionality constant associated with the intrinsic optical anisotropy of the system. Such a concentration scaling, as shown in Figures 4b and 5b, does indeed collapse all steady-state data onto two master curves. The solid lines in these plots are the DEMG model calculations using infinite series expansion as described in part 1.[4] The values for the parameters needed for the numerical calculations are $c_1 = 0.78$, $c_2 = 0.20$, $c_3 = 0.02$, $L_1 = 0.7538$, $L_2 = 1.508$, and $L_3 = 2.261$. Here, the subscripts 1–3 are used to denote collagen monomers, dimers, and trimers, respectively. c_i is the number concentration (normalized by the total number concentration c) for rods with length L_i, and L_i has been normalized by the appropriate average rod length, $(\sum c_i L_i^2)^{1/2}$. Quantitative fitting of the model predictions to the data requires two adjustable parameters, M and β, in which β is the proportionality factor needed to equate the rotational diffusivity D_r to c_i and L_i. For a monodisperse system, the relation suggested by the Doi–Edwards model is

$$D_r = \beta(cL^3)^{-2}D_{r0} \tag{4}$$

where D_{r0} is the rotational diffusivity for a single, untangled rod. For a polydisperse system, the expression is more complicated and is written as eq 15 and 18 of part 1.[4] Figures 4 and 5 show that the steady-state data agree very well quantitatively with the DEMG model in spite of the limited flexibility of collagen. The original Doi-Edwards model, on the other hand, yields a poorer quantitative agreement with the results.

Figures 6 and 7 show the transient flow data following the inception of shear for six different shear rates ranging from $g/D_r = 1.56$ to 250. In Figure 6, Δn has been normalized by the steady-state value at that shear rate, Δn_{ss}. Time t has been normalized by the characteristic time D_r^{-1}. There are no additional adjustable parameters for fitting the transient flow data besides β and M, which are the same ones obtained from fitting the steady-state data. Upon the inception of shear, the collagen results indicate that the birefringence overshoots before it reaches steady state at all shear rates studied. The DEMG model, on the other hand, predicts no overshoot when g/D_r is less than or near unity. Moreover, the magnitude of the overshoot measured experimentally is always higher than the model prediction at any given shear rate. Figure 8 plots the magnitude of the overshoot vs. g/D_r, with the model prediction denoted by the solid line. The overshoot measured for the rat tail tendon collagen is 3–6% higher than the model predictions over a large range of shear rate. This "excess" in the overshoot is believed to be a direct measure of the flexibility of the molecule. A flexible molecule can be deformed by extension of its coiled configuration in addition to the orientation effects of the flow, which is the only form of flow response for a perfectly rodlike molecule. The overshoot in Δn for rat tail tendon collagen is still small compared to other more flexible systems, however. A previous study on xanthan gum, a double-stranded helical molecule that has a less rigid structure than the triple-stranded collagen, indicated an overshoot in Δn as high as 50%.[24] Flexible polymers such as polystyrene, on the other hand, produce overshoots of 200% or more at high shear rates.[27]

As summarized in a double-logarithmic plot of Figure 9, the time predicted for the maximum in the overshoot is slightly shorter than that measured for the rat tail tendon collagen. The agreement is nonetheless quite good over the whole range of shear rates. The time-dependent angle (Figure 7) exhibits an undershoot following the inception of strong shear by both the model and the data. The overall trend of Figures 6 and 7 indicates that quantitative fitting of the model to the data is better at high shear rates than at low shear rates.

Figure 10 shows plots of the relaxation of the birefringence following the cessation of shear. As is predicted by the DEMG model for a polydisperse system, the relaxation data show multiple relaxation times—a rapid initial drop followed by a slower decay. This trend is not predicted for a monodisperse solution described by the original Doi–Edwards model, which is characterized by a single relaxation time. The faster decay results from the relaxation of the monomers which are governed by a higher value of D_r, and the slower decay is due to the relaxation of the dimers and the trimers. Quantitative comparison of the model to the data is good at high shear rates, especially at short times. The agreement worsens as the shear rate decreases. This series of plots shows that the model predicts a weak shear rate dependence of the relaxation rates, while the measurements indicate that the relaxation rates are strongly dependent on shear rate.

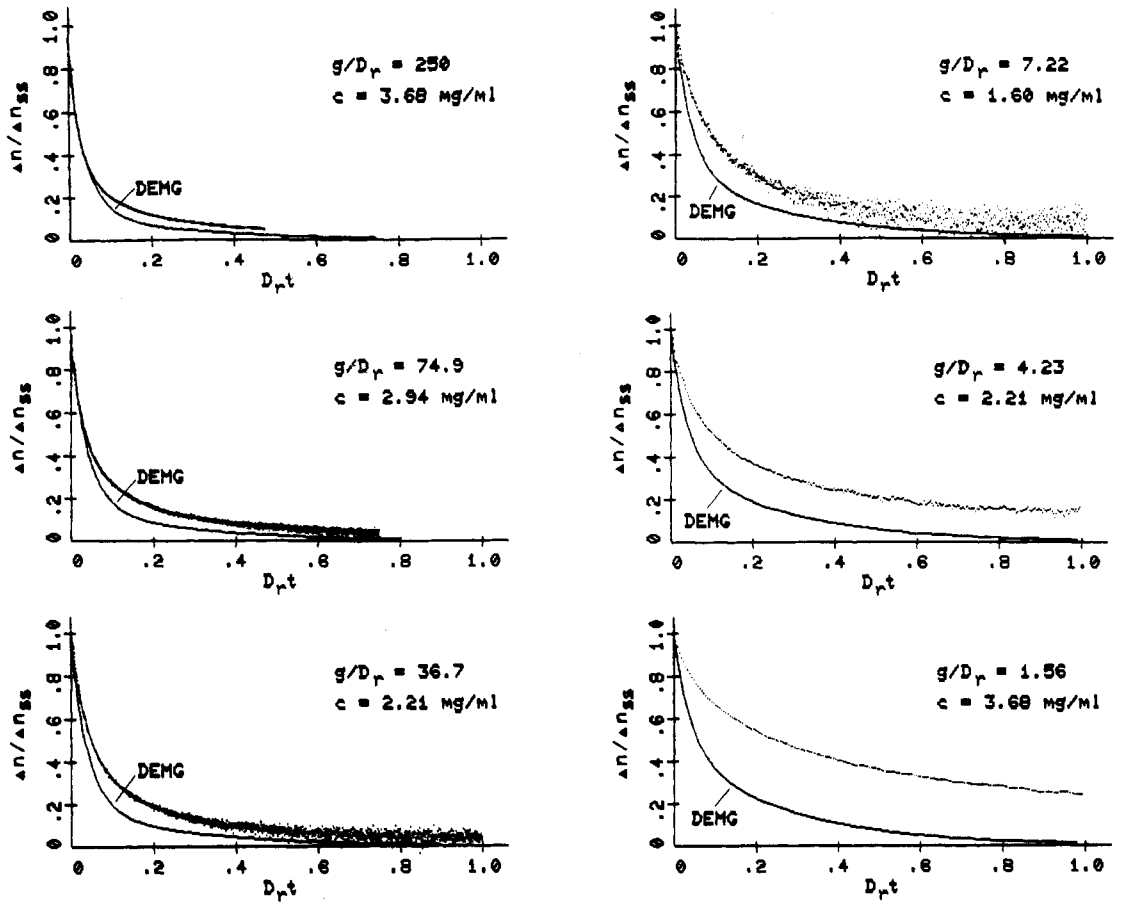

Figure 10. Birefringence normalized by the steady-state value as a function of the dimensionless time following the cessation of shear flow for the rat tail tendon collagen solutions. The lines denoted by DEMG are the model calculations.

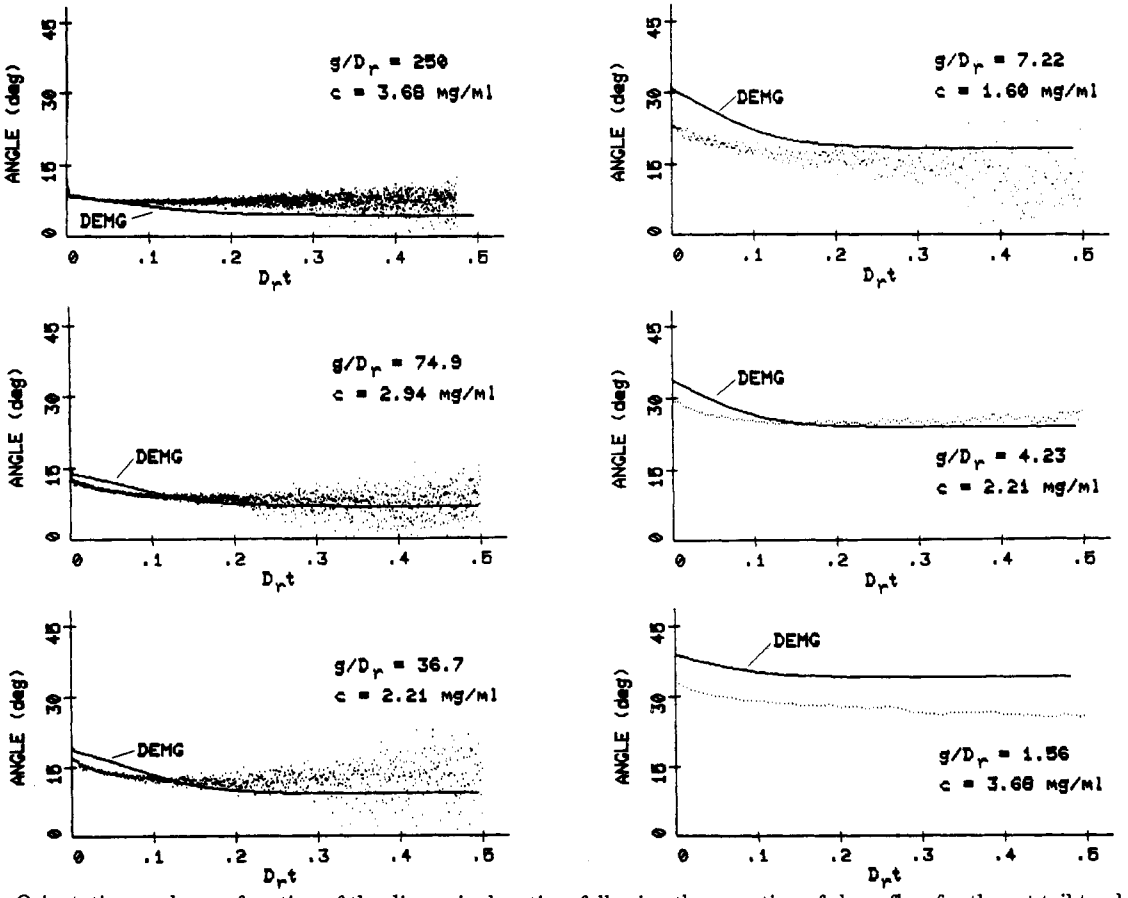

Figure 11. Orientation angle as a function of the dimensionless time following the cessation of shear flow for the rat tail tendon collagen solutions. The lines denoted by DEMG are the model calculations.

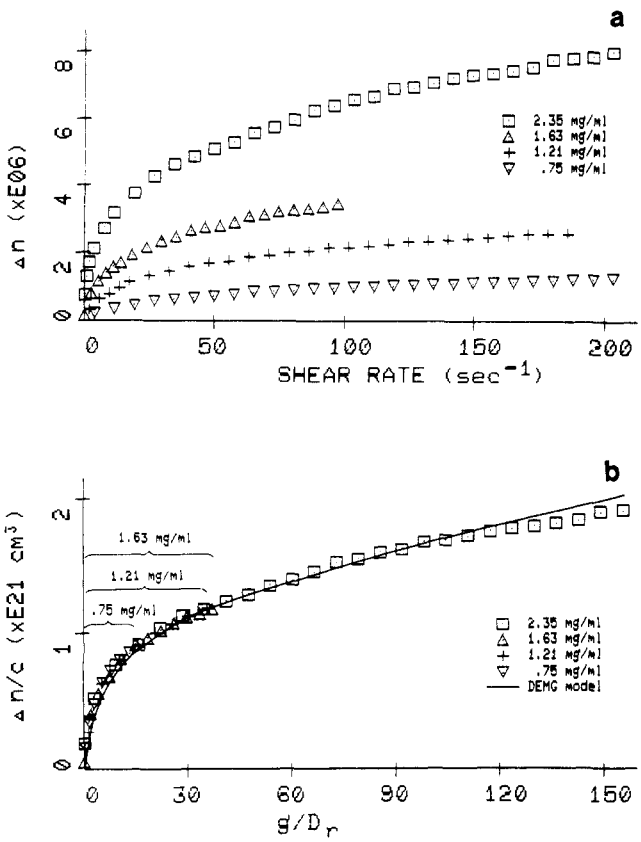

Figure 12. (a) Steady-state birefringence vs. the applied shear rate for four bovine collagen solutions. (b) Same set of data reduced by the concentration scaling suggested by the DEMG model.

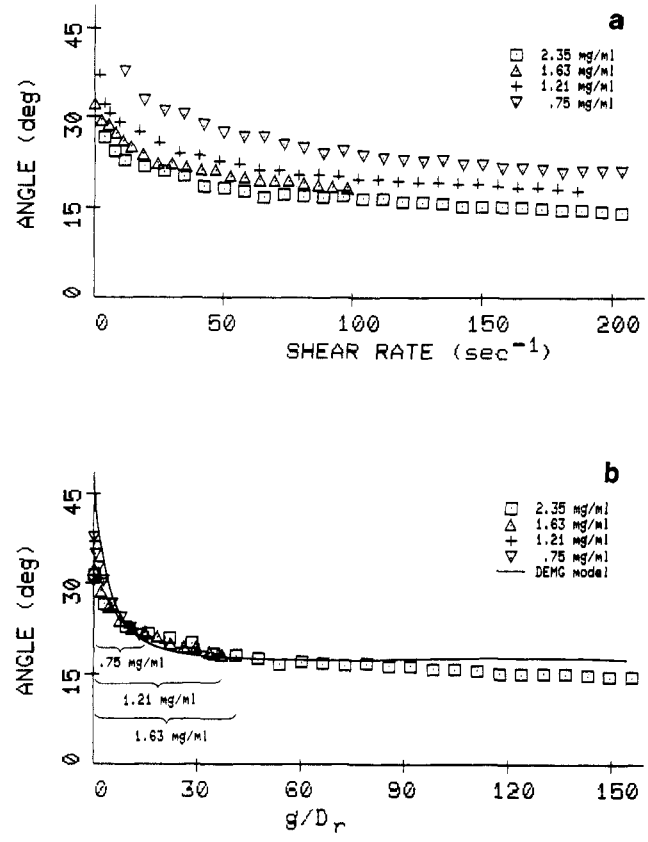

Figure 13. (a) Steady-state orientation angle vs. the applied shear rate for four bovine collagen solutions. (b) Same set of data reduced by the concentration scaling suggested by the DEMG model.

Figure 11 is the time-dependent orientation angle following the cessation of flow. The angle decreases slightly during the relaxation process at all shear rates. This phenomenon is not predicted for a monodisperse system because the drop in the angle is again a result of the multiple relaxation times characterizing the system. Since the monomers are disoriented by the Brownian motion faster than the dimers and the trimers, the average orientation angle drops with time during relaxation toward the orientation of the longer rods, which are oriented at lower angles than the monomers. Consequently, the original Doi–Edwards model is not adequate for describing the dynamics of collagen since it predicts the angle to remain constant at the value prior to the cessation of flow during relaxation.[4] The relaxation results also indicate a better quantitative agreement between the DEMG model and the data at higher values of g/D_r.

Bovine Collagen—Bimodal System. The flow birefringence measurements of the bovine collagen solutions are compared to the DEMG model for bimodal systems using parameters $c_1 = 0.85$, $c_2 = 0.15$, $L_1 = 0.8305$, and $L_2 = 1.661$. Four solutions with concentrations ranging from 0.75 to 2.36 mg/mL have been studied. Figures 12a and 13a are plots of the steady-state birefringence and orientation angle, and Figures 12b and 13b show the same set of data reduced by the concentration as described in eq 2 and 3. The solid lines are the DEMG model predictions, which are fitted to the reduced data by adjusting M and β.

Figure 14 shows plots of the time-dependent Δn following the inception of shear for six shear rates covering $g/D_r = 0.319$–31.9. The magnitude of the overshoot is always higher than the model prediction at any value of g/D_r as in the case of rat tail tendon collagen. The percent overshoot as a function of the applied shear rate is summarized in Figure 15. This graph indicates a 10% excess overshoot of the birefringence for the bovine collagen solutions over the range of shear rates studied. If we compare this plot to Figure 8, the bovine collagen appears to be less rigid than the rat tail tendon collagen, which overshoots 3–6% over the model predictions. Figure 16 summarizes the temporal position of the maximum of the overshoots double-logarithmically. This plot shows that the data also agree quite well with the model prediction (solid line). The time-dependent orientation angle following the inception of shear, as shown in Figure 17, exhibits undershoot at higher shear rates by the model but only slightly by the data.

Results following the cessation of shear are shown in Figures 18 and 19. The relaxation of the normalized birefringence (Figure 18) is again characterized by two distinct relaxation times as is predicted by the DEMG model. Quantitative comparison of the model to the data, however, is not as successful, especially at lower shear rates. The data indicate longer relaxation times for both the monomers and the dimers. The orientation angle, shown in Figure 19, exhibits a decrease by both the data and the model upon the cessation of shear as a result of polydispersity.

Discussion

Both the steady-state and the transient flow data indicate that the concentration scaling (c^{-2} dependence of D_r) predicted by the Doi–Edwards model is indeed correct. The inverse-square dependence on the concentration means that two-body collisions are the dominant mechanism for steric hindrance.

The adjustable parameter, M, which is associated with the intrinsic anisotropy of the polarizability of collagen in

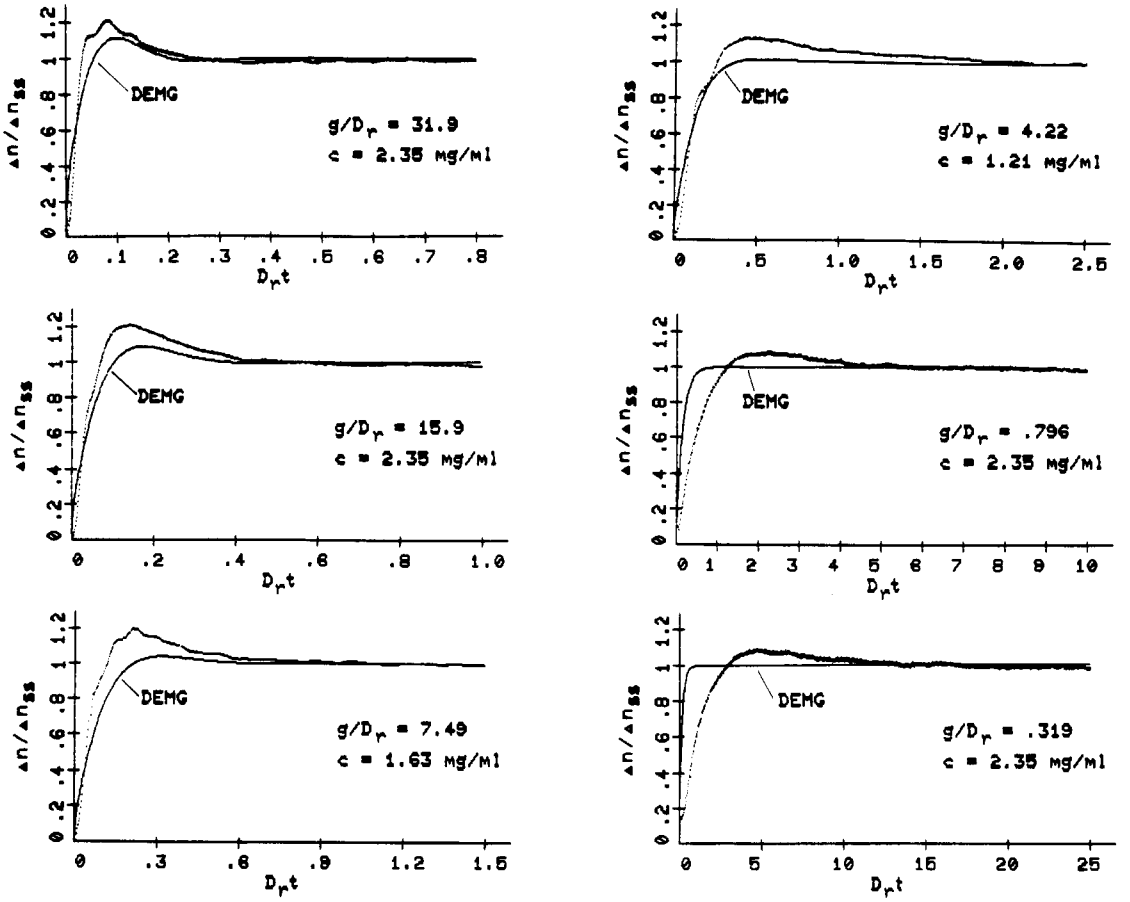

Figure 14. Birefringence normalized by the steady-state value as a function of the dimensionless time following the inception of shear flow for the bovine collagen solutions. The lines denoted by DEMG are the model calculations.

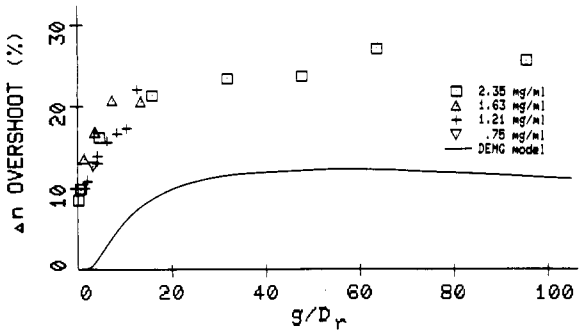

Figure 15. Percent overshoot in birefringence upon the inception of shear flow vs. the dimensionless shear rate for the bovine collagen solutions.

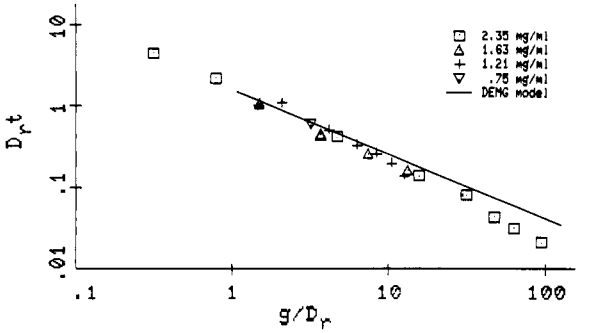

Figure 16. Double-logarithmic plot of the temporal positions of the overshoot in birefringence upon the inception of shear flow vs. the dimensionless shear rate for the bovine collagen solutions.

glycerin–water, is found to be 7.7×10^{-21} cm^3 for the rat tail tendon collagen and 7.2×10^{-21} cm^3 for the bovine collagen. When these values are normalized by the corresponding characteristic length, the constant M is 5.8×10^{-21} cm^3 for monomeric rat tail tendon collagen and 6.0×10^{-21} cm^3 for monomeric bovine collagen. Within experimental errors, these two values for M are essentially identical, which is expected since both collagen samples contain mostly (at least 95%) type I collagen.

The values of the second adjustable parameter β are 6×10^6 and 3×10^6 for the rat tail tendon and bovine collagen solutions, respectively. These values are much larger than a value of approximately $O(1)$ anticipated by Doi and Edwards.[5] High values of β have been reported for rodlike macromolecules in the past by others studying steady-state flows and several possible explanations have been proposed.[28,29] Most explanations suggest that the rods do not have to traverse their entire length in order to remove the steric hindrance between adjacent rods. Because of the very strong dependence of the diffusion coefficent on rod length ($O(L^{-9})$), any small decrease in the effective length scale to induce rotational hindrance will dramatically increase the value of β. Flexibility also tends to reduce the effective rod length, thereby increasing the value of β.

The DEMG model has been found to successfully predict the flow behaviors of the polydisperse collagen solutions under both steady and transient flow conditions. Properties unique for polydisperse systems that are predicted only by the DEMG model but not by the Doi–Edwards model have been observed experimentally. For example, the steady-state angle levels off at moderate shear rate regions instead of decreasing monotonically with shear rate to zero (see Figures 5 and 13). This is due to the much lower effective rotational diffusivities of the longer rods in a polydisperse solution. Consequently, the effective shear rate experienced by the long chains is always higher

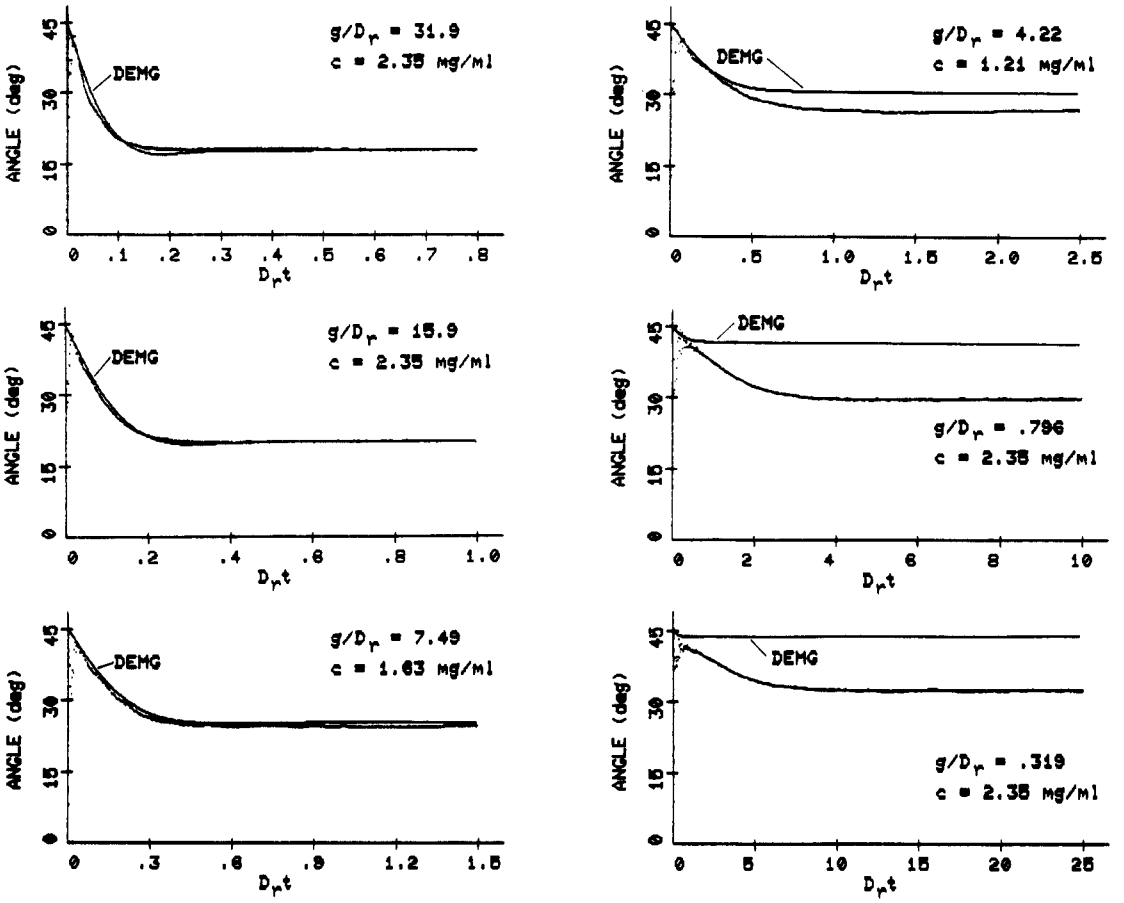

Figure 17. Orientation angle as a function of the dimensionless time following the inception of shear flow for the bovine collagen solutions. The lines denoted by DEMG are the model calculations.

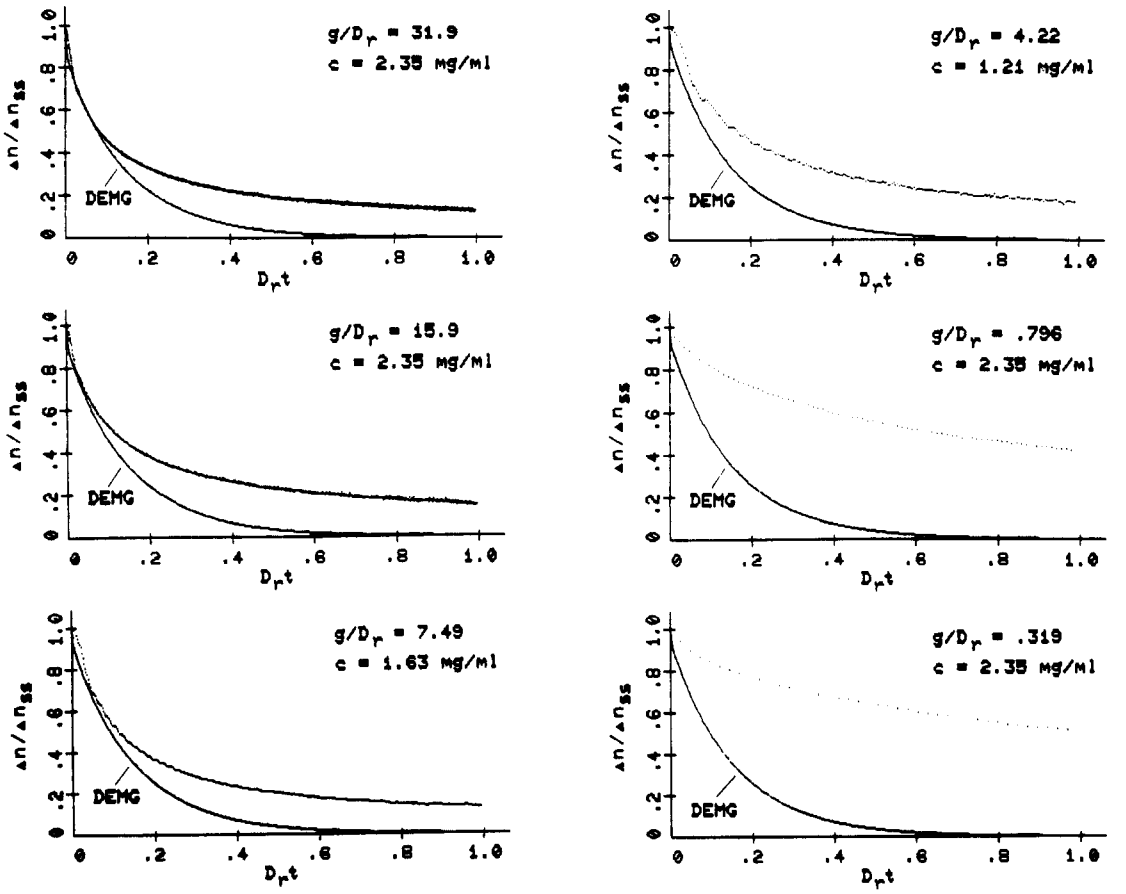

Figure 18. Birefringence normalized by the steady-state value as a function of the dimensionless time following the cessation of shear flow for the bovine collagen solutions. The lines denoted by DEMG are the model calculations.

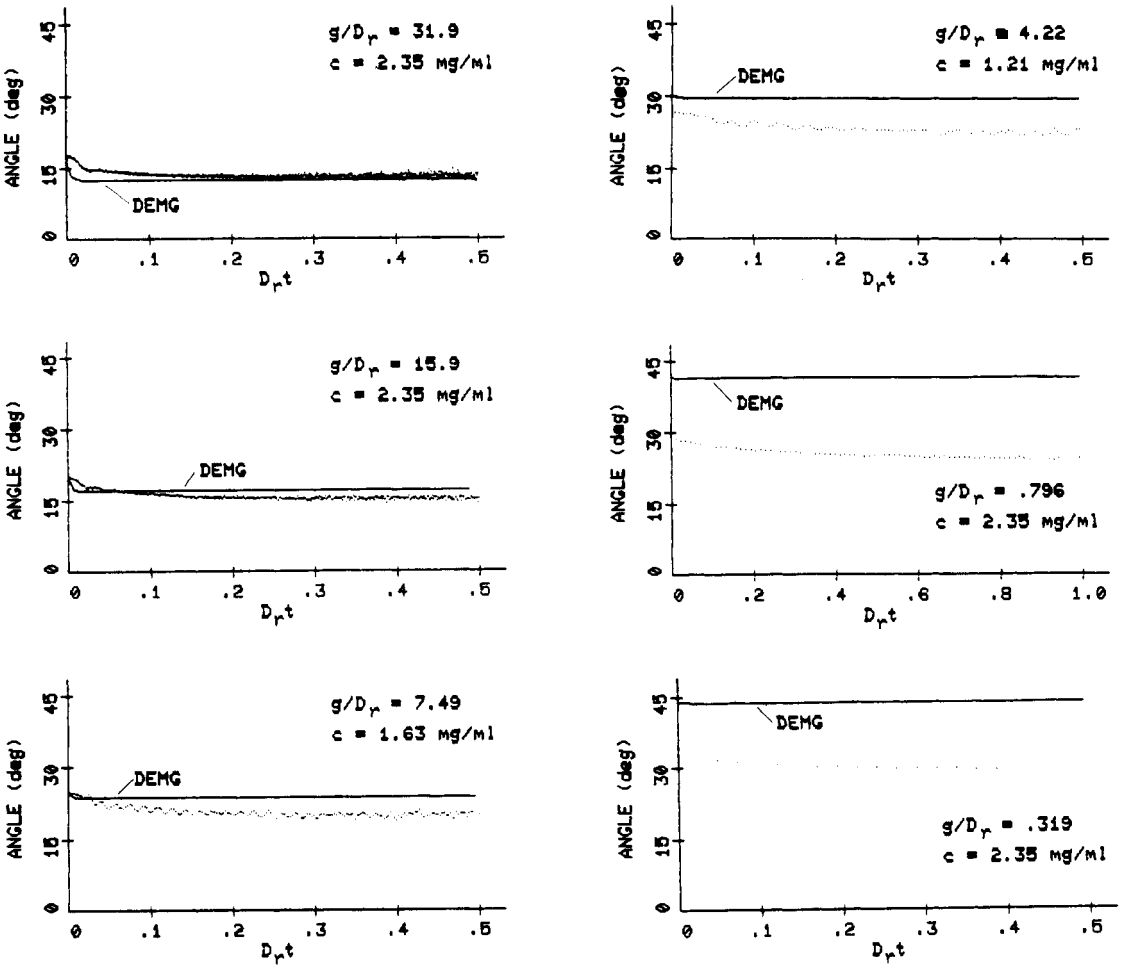

Figure 19. Orientation angle as a function of the dimensionless time following the cessation of shear flow for the bovine collagen solutions. The lines denoted by DEMG are the model calculations.

at any given value of g/D_r. At low shear rates where the short rods are only slightly oriented by the flow, the overall flow dynamics are dominated by the long rods. At higher shear rates were the flow effect saturates for the long rods, the dynamics of the short rods begin to dominate. At this point, the angle starts to level off or even increase toward the orientation of the shorter rods which are oriented at a higher angle than the longer rods.

The effects of polydispersity are especially important in the cessation of flow results. The multiple relaxation times characterizing a polydisperse system are responsible for the decrease in the orientation angle measured during the relaxation process (Figures 11 and 19). The birefringence also relaxes with more than one relaxation rate as shown in Figures 10 and 18.

Quantitatively, model comparison has been found to be good with the steady state and the inception of shear flow results, and fair with the relaxation results. Moreover, data obtained at higher shear rates provide better agreement with the model. We attribute most of these quantitative disparities to the finite but limited flexibility of the collagen structure. At very low shear rates, in particular, the applied flow field has very little effect on the equilibrium conformation of the slightly flexible molecules and therefore the flow dynamics deviate more from that predicted by the DEMG model, which describes perfectly rodlike systems. At higher shear rates, on the other hand, the flow tends to extend the molecule closer to a rodlike configuration, thereby improving the fit with the model.

The limited flexibility possessed by the collagen molecules is directly indicated by the magnitude of the overshoot in birefringence following the inception of shear flow. Both samples produce overshoots with magnitude close to but slightly higher than that predicted by the model. The bovine collagen, however, was found to yield a higher overshoot than the rat tail tendon collagen, which suggests that the former sample is somewhat less rigid than the latter. The higher degree of flexibility could be the result of the pepsin treatment used to remove the telopeptides in isolating the bovine collagen from the source. Pepsin digestion, not used in preparing the rat tail tendon collagen, could cause incomplete cleaving of the telopeptides, resulting in a more flexible cross-link for the dimeric molecules. Moreover, it has been suspected to cause a trace amount of imperfect helices possibly nicked at about 225 nm from the N-terminal end of the helix since this is the site for attack by vertebrate collagenase.[30] Another possible explanation for the difference in flexibility is mechanical degradation by high flow rate pumps used to handle the commercially manufactured bovine collagen. The rat tail tendon collagen, on the other hand, was prepared on a test tube scale and therefore has escaped such treatment.

In general, data obtained on the more rigid rat tail tendon collagen are in better agreement with the DEMG model. For example, following the inception of shear the rat tail tendon collagen produces undershoots in the orientation angle very similar to the model predictions (Figure 7). The bovine collagen, on the other hand, yields a much smaller undershoot (Figure 17). Furthermore, the relaxation data also show better agreement for the rat tail tendon collagen solutions. Since increasing the flexibility

increases the disparity, it is a good indication that the limited flexibility of the molecules is responsible for the remaining discrepancies between the experimental results and the DEMG model. The effects of chain flexibility will be studied more thoroughly in another paper focused solely on this subject.[31]

Concluding Remarks

We conclude that the effects of polydispersity on the flow dynamics of semidilute rodlike systems are adequately described by the DEMG model. The remaining quantitative discrepancies between the data and the model could largely be due to the limited flexibility of the systems used for this study. Recently we have devised a new procedure by which more rodlike collagen molecules can be prepared by reducing the contour length close to the persistence length. This new preparation procedure will allow us to vary the rigidity of the molecules and hence offer an opportunity to study the effects of limited flexibility directly by experiment. This study will be reported in a forthcoming paper.

Acknowledgment. This research is funded by the NSF-MRL Program through the Center for Materials Research at Stanford University and partially supported by the National Science Foundation (Grant No. NSF-CPE80-25833), the National Institutes of Health (Grant No. RO-1-HL28373), and the ARCO Foundation. We thank Collagen Corp. of Palo Alto, CA, for generously providing us with the collagen samples. The technical assistance of Dr. R. Condell is also gratefully acknowledged.

References and Notes

(1) Black, W. B. In "Flow Induced Crystallization in Polymer Systems"; Millar, R. L., Ed.; Gordon and Breach: New York, 1977.
(2) Yannas, I. V.; Burke, J. F.; Gordon, P. L.; Huang, C. U.S. Patent 4 060 081, 1977.
(3) Kaplan, E. N.; Falces, E.; Tolleth, H. *Ann. Plast. Surgery* **1983**, *10*, 437.
(4) Chow, A. W.; Fuller, G. G. *Macromolecules*, preceding article in this issue.
(5) Doi, M.; Edwards, S. F. *J. Chem. Soc., Faraday Trans. 2* **1978**, *74*, 560, 918.
(6) Marrucci, G.; Grizzuti, N. *J. Polym. Sci., Polym. Lett. Ed.* **1983**, *21*, 83. Marrucci, G.; Grizzuti, N. *J. Non-Newtonian Fluid Mech.* **1984**, *14*, 103.
(7) Eyre, D R. *Science (Washington, D.C.)* **1980**, *207*, 1315.
(8) Nestler, F. H. M.; Hvidt, S.; Ferry, J. D.; Veis, A. *Biopolymers* **1983**, *22*, 1747.
(9) Saito, T.; Iso, N.; Mizuno, J. H.; Onda, N.; Yamato, H.; Odashima, H. *Biopolymers* **1982**, *21*, 715.
(10) Hoffmann, H.; Voss, T.; Kuhn, K.; Engel, J. *J. Mol. Biol.* **1984**, *172*, 325.
(11) Chandrakasan, G.; Torchia, K. A.; Piez, K. A. *J. Biol. Chem.* **1976**, *251*, 6062.
(12) Drake, M. P.; Davidson, P. F.; Bump, S.; Schmitt, F. O. *Biochemistry* **1966**, *5*, 301.
(13) Daniels, J. R.; Knapp, T. R. U.S. Patent 3 949 073, 1974.
(14) Luck, E. E.; Daniels, J. R. U.S. Patent 4 140 537, 1976.
(15) Luck, E. E.; Daniels, J. R. U.S. Patent 4 233 360, 1978.
(16) Laemmli, U. K. *Nature (London)* **1970**, *227*, 680.
(17) Morrissey, J. H. *Anal. Biochem.* **1981**, *117*, 307.
(18) Gornall, A. G.; Bardawill, C. J.; David, M. M. *J. Biol. Chem.* **1949**, *177*, 751.
(19) Furthmayr, H.; Madri, J. A. *Collagen Relat. Res.: Clin. Exp.* **1982**, *2*, 349.
(20) Shotton, M. M.; Burke, B.; Branton, D. *J. Mol. Biol.* **1979**, *131*, 303.
(21) Engel, J.; Odermatt, E.; Engel, A.; Madri, J. A.; Furthmayr, H.; Rohde, H.; Timpl, R. *J. Mol. Biol.* **1981**, *150*, 97.
(22) Gortemaker, F. G.; Hansen, M. B.; de Cindo, B.; Laun, H. M.; Janeschitz-Kriegl, H. *Rheol. Acta* **1976**, *15*, 242, 256.
(23) Osaki, K.; Bessho, N.; Kojimoto, T.; Kutata, M. *J. Rheol.* **1979**, *23*, 457.
(24) Chow, A. W.; Fuller, G. G. *J. Rheol.* **1984**, *28*, 23.
(25) Chow, A. W.; Fuller, G. G., submitted for publication in *J. Non-Newtonian Fluid Mech.*
(26) Oriel, P. J.; Schellman, J. A. *Biopolymers* **1966**, *4*, 469.
(27) Zebrowski, B. E.; Fuller, G. G., submitted for publication in *J. Polym. Sci., Polym. Phys. Ed.*
(28) Jain, S.; Cohen, C. *Macromolecules* **1981**, *14*, 759.
(29) Odell, J. A.; Atkins, E. D. T.; Keller, A. *J. Polym. Sci., Polym. Lett. Ed.* **1983**, *21*, 289.
(30) Gross, J.; Harper, E.; Harris, E. D., Jr.; McCroskery, P.; Highberger, J. H.; Corbett, C.; Kang, A. H. *Biochem. Biophys. Res. Commun.* **1974**, *61*, 605.
(31) Chow, A. W.; Fuller, G. G.; Wallace, D. G.; Madri, J. A. *Macromolecules*, following paper in this issue.